MAE 598 Design Optimization

Design Optimization of a Shell and Tube Heat Exchanger

Harikirupakar Kishore Kumar
Prajwal Nagaraj
Rohan Halageri Uday

ACKNOWLEDGEMENT

The authors would like to sincerely thank Dr. Yi Ren for his continuous guidance, comments during the progress of the project and most importantly for providing the opportunity to work on this project.

The authors would also like to extend their gratitude to Mr. Donley Hurd for his timely support and the facilities at the CAD/CAM lab at Goldwater Center, Arizona State University.

Table of Contents

Abstract

This project presents an attempt to optimize a shell and tube heat exchanger. Heat exchanger is a device used to transfer heat between two or more fluids. Of the various types of heat exchangers used in various industries, the shell and tube heat exchanger is probably the most versatile and widely used in most industrial sectors. This project captures the optimization of the total annual operating cost together with structural and CFD optimization. Thus, an attempt has been made to obtain a set of optimum dimensions of the heat exchanger subject to a given set of inlet and desired outlet conditions. Optimization of the heat exchanger was carried out in three stages: thermal analysis using a mathematical model; optimization of the nozzle considering structural loads using ANSYS; and CFD analysis using ANSYS. All parameters have been taken from the relevant industry codes and standards, thus making the optimization problem akin to a real-world scenario.

Introduction

The approach used in the optimization was a series optimization approach where the outputs of the mathematical model acted as inputs to the structural and CFD analysis. An attempt was also made to highlight the sensitivity of the design variables on objective functions thus illustrating the relative significance of the design variables in the optimization problem.

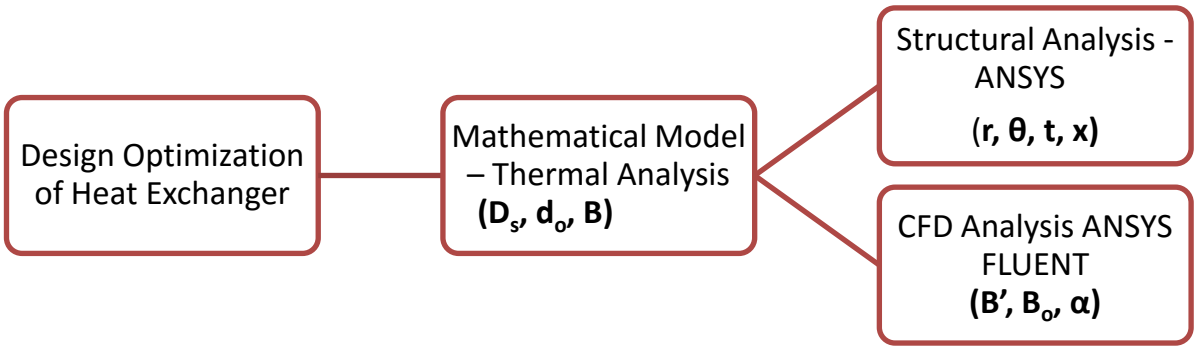

Figure 1: Schematic of System integration

Subsystem 1: Mathematical Modelling of the heat exchanger

1. Problem Statement

A mathematical model for minimizing the annual cost incurred in the operation of a heat exchanger has to be formulated and optimized. The thermal and the physical properties of the two fluids at the inlet conditions are known. It is desired that the heat exchanger be designed for given outlet temperatures of both the shell-side and tube-side fluids. The required heat transfer area and pumping capacity to achieve the desired temperature conditions have been computed as a function of the design variables. The objective function is a function of the effective heat transfer area and the pumping power required to overcome the pressure drop.

2. Nomenclature

a_1	numerical constant (\$)
a_2	numerical constant (\$/m^2)
a_3	numerical constant
A	heat exchanger surface area (m^2)
B	baffle spacing (m)
C	numerical constant
C_e	energy cost (\$/kWh)
C_i	capital investment (\$)
C_0	annual operating cost (\$)
C_i	total discounted operating cost (\$)
C_p	specific heat (J/kgK)
C_{tot}	total annual cost (\$)
d_e	equivalent shell diameter (m)
d_i	tube inner diameter (m)
d_o	tube outer diameter (m)
D_s	shell inside diameter (m)
F	temperature difference correction factor
H	annual operating time (hrs)
h_s	shell side convective coefficient (W/m^2K)
h_t	tube side convective coefficient (W/m^2K)
i	annual discount rate (%)
k	thermal conductivity (W/mK)
L	tube length (m)
LMTD	logarithmic mean temperature difference (K)
m_s	shell side mass flow rate (kg/s)
m_t	tube side mass flow rate (kg/s)

n	number of tube passes
n_1	numerical constant
N_t	number of tubes
P	pumping power (W)
P_s	internal fluid pressure ($barg$)
Pr_s	shell side Prandtl number
Pr_t	tube side Prandtl number
Re_s	shell side Reynold's number
Re_t	tube side Reynold's number
R_{fs}	shell side fouling resistance
R_{ft}	tube side fouling resistance
S_t	tube pitch (m)
T_{ci}	cold fluid inlet temperature (K)
T_{co}	cold fluid outlet temperature (K)
T_{hi}	hot fluid inlet temperature (K)
T_{ho}	hot fluid outlet temperature (K)
U	overall heat transfer coefficient (W/m^2K)
v_s	shell side fluid velocity (m/s)
v_t	tube side fluid velocity (m/s)
ΔP	pressure drop (Pa)
$\Delta P_{tubeelbow}$	tube elbow pressure drop (Pa)
$\Delta P_{tubelengt\ h}$	tube length pressure drop (Pa)
μ	dynamic viscosity ($Pa-s$)
ρ	density (kg/m^3)

3. Mathematical Models

The mathematical model has been constructed considering the principles of heat transfer and fluid mechanics[1][2][3]. The equation relating the design variables to other parameters and constraints are as follows:

A.Heat transfer

i) Tube side heat transfer coefficient:

$$h_f = \left(\frac{k_t}{d_i}\right)\left(3.657 + \frac{\left(0.0677 * Re_t * Pr_t * \left(\frac{d_i}{L}\right)\right)^{1.33^{0.33}}}{1 + 0.1 * Pr_t * \left(Re_t * \left(\frac{d_i}{L}\right)\right)^{0.3}}\right)$$

(if Re_t<2300)

$$h_f = \left(\frac{k_t}{d_i}\right)\frac{\left(\left(\frac{f_t}{8}\right) * (Re - 1000)Pr_t\right)}{\left(1 + 12.7\left(\frac{f_t}{8}\right)^{0.5} * \left(Pr_t^{0.667} - 1\right)\right)}\left(1 + \frac{d_i}{L}\right)^{0.67}$$

(if $2300<Re_t<10000$)

$$h_f = 0.027 * \frac{k_t}{d_o} * Re_t^{0.8} * Pr_t^{0.667} * \left(\frac{\mu_t}{\mu_{wt}}\right)^{0.14}$$

(if $Re_t>10000$)

Where,

$$f_t = (1.82\log 10^{Re_t} - 1.64)^{-2}$$

$$Re_t = \frac{\rho_t * v_t * d_i}{\mu_t}$$

$$v_t = \frac{m_t}{0.25\Pi * d_t^2 * \rho_t} * \left(\frac{n}{N_t}\right)$$

$$N_t = c\left(\frac{D_s}{d_o}\right)^{n_1} \quad Pr_t = \frac{(\mu_t * c_{pt})}{k_t} \quad d_i = 0.8d_0$$

ii) shell side heat transfer coefficient:

$$h_s = \frac{0.36 * k_t}{d_e} * Re_s^{0.55} * Pr_s^{0.33} * \left(\frac{\mu_s}{\mu_{wts}}\right)^{0.14}$$

$$d_e = 4 * \frac{S_t^2 - (\Pi * 0.25 * d_0^2)}{\Pi d_0}$$

$$d_e = 4 * \frac{0.43S_t^2 - (\Pi * 0.5 * d_0^2)}{0.5\Pi d_0}$$

$$A_s = D_s B\left(1 - \frac{d_o}{S_t}\right)$$

$$V_s = \frac{m_s}{\rho_s A_s} \qquad Re_s = \frac{m_s d_e}{A_s \mu_s} \quad Pr_s = \frac{\mu_s C_{ps}}{k_s}$$

$$U = \frac{1}{\left(\frac{1}{h_s}\right) + R_{fs} + \left(\frac{d_o}{d_i}\right)\left(R_{ft} + \left(\frac{1}{h_t}\right)\right)}$$

iv) LMTD

$$LMTD = \frac{(T_{hi\,-}\,T_{co}) - (T_{ho} - T_{ci})}{\ln((T_{hi\,-}\,T_{co})/(T_{ho} - T_{ci}))}$$

v) Correction Factor

$$F = \sqrt{\frac{R^2 - 1}{R - 1}} * \frac{\ln((1-P)(1-PR))}{\ln((2 - PR + 1 - \sqrt{R^2 + 1})/(2 - PR + 1 + \sqrt{R^2 + 1})}$$

Where R, Correction coefficient is

$$R = \frac{(T_{hi\,-}\,T_{ho})}{(T_{co\,-}\,T_{ci})}$$

And P, Efficiency is

$$P = \frac{(T_{co\,-}\,T_{ci})}{(T_{ho\,-}\,T_{ci})}$$

vi) Heat-exchangersurface area

$$A = \frac{Q}{U * F * LMTD}$$

Where $Q = m_h * Cp_h * (T_{hi\,-}\,T_{ho}) = m_c * Cp_c * (T_{co\,-}\,T_{ci})$

vii) Tube Length

$$L = \frac{A}{\pi d_o N_t}$$

B. <u>Pressure Drop</u>

i) Tube side pressure drop

$$\Delta P_t = \Delta P_{tube\,\_\,length} + \Delta P_{tube\,\_\,elbow}$$

$$\Delta P_t = \frac{\rho_t v_t^{\,2}}{2} * (\frac{L}{d_i}\, f_t + p)n$$

Where, p =4.5

ii) Shell side pressure drop

$$\Delta P_s = f_s(\frac{\rho_s v_s^2}{2})(\frac{L}{B})(\frac{D_s}{D_e})$$

Where,

$$f_s = 2b_o \mathrm{Re}_s^{-0.15} \quad b_0 = 0.72$$

iii) Pumping power

$$P = \frac{1}{\eta}(\frac{m_t}{\rho_t}\Delta P_t + \frac{m_s}{\rho_s}\Delta P_s)$$

C. Objective Function

$$C_{tot} = C_i + C_{od}$$

$$C_i = a_1 + a_{2A}A^{a_3}$$

For stainless steel heat exchanger

$$a_1 = 8000 \qquad a_2 = 259.2 \quad a_3 = 0.93$$

$$C_{od} = \sum_{x=1}^{n1} \frac{C_o}{(1+i)^x}$$

$$C_o = PC_eH$$

$$H = 7000\ hrs$$

D. Constraints

The constraints acting on the systems are the inlet and outlet conditions of the shell side and tube side fluids. These act as equality constraints and are as follows:

$$h_1 = T_{si} \qquad h_2 = T_{so} h_3 = T_{ti} h_4 = T_{to}$$

$$g_1: lb \le D_s \le ub \qquad g_2: lb \le d_o \le ub g_3: lb \le B \le ub$$

4. Model Analysis

The above mathematical model is a complex model with three design variables of inside shell diameter (D_s), outside tube diameter (d_o) and baffle spacing (B).The objective cost function is a

function of the effective heat transfer area and pumping power. Pumping power would be determined by the quantum of pressure drop experienced by the fluids both on the shell side and tube side. Greater effective surface area would be highly desirable in terms of maximizing the heat transfer between the two fluids but simultaneously higher surface area would lead to greater pressure drop, thus leading to a higher required pumping power. Thus, there exists an obvious trade-off between the two parameters. The effective heat transfer area and the pumping power are functions of the design variables.

5. Discussion of Results

The mathematical model has been solved through the 'fmincon' with SQP algorithm in MATLAB. The MATLAB code for the same has been appended in the report.

To solve the mathematical model, a sample case of heat transfer between kerosene (shell-side fluid) and crude oil (tube-side fluid) has been considered. The inlet & outlet conditions of the two fluids along with their thermo-physical properties have been illustrated in Table 1.

Table 1: Process input and physical parameters for sample case study

	Fluid	**Mass Flow (kg/s)**	**T_i (°C)**	**T_o (°C)**	**ρ (kg/m^3)**	**c_p (kJ/kg-K)**	**μ (Pa-s)**	**k (W/m-K)**
Shell Side	Kerosene	5.52	199.00	93.30	850.00	2.47	0.0004	0.13
Tube Side	Crude Oil	18.80	37.80	76.70	995.00	2.05	0.00358	0.13

Further, the design variables have been bounded with the earlier mentioned inequality constraints:

$$g_1: 0.2 \leq D_s \leq 2 \qquad g_2: 0.015 \leq d_o \leq 0.051 \qquad g_3: 0.2 \leq B \leq 0.5$$

The solution to the mathematical model in its present form takes 24 iterations. The solution obtained for the optimum value of the design variables are as follows:

$$D_s = 1.0545 \qquad d_o = 0.0459 \qquad B = 0.5000$$

and the value of the objective cost function at the optimum value of design variables is,

$$C = 18429.4$$

The plot of function value v/s number of iterations is presented in Figure 1.

As the optimal value for baffle spacing is at its upper bound, it appears that function is monotonic with respect to the design variable ‘B’. However, this is not the case, as if we increase the baffle spacing to values greater than 0.565, the optimal value for ‘B’ no longer lies on the upper bound. This shows that the optimization problem is well constrained.

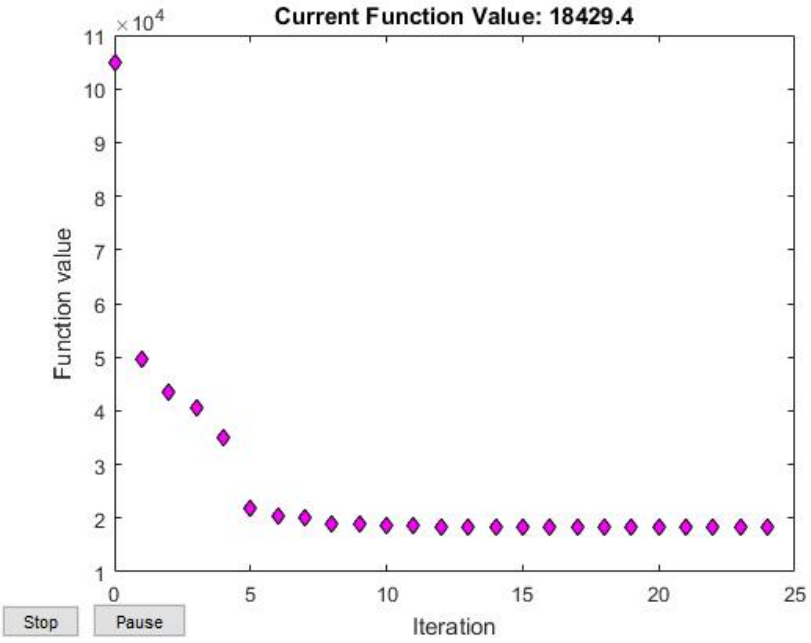

Figure 1.1 : Plot of function values v/s number of iterations

References

[1] Cengel A.Y, “Fundamentals of heat transfer, 6th edition (2009)”; John Wiley & Sons

[2] Bejan A, “Convection heat transfer, 3rd edition (2004)”; Wiley Publications

[3] Ponce-Ortega J.M et. al., “Design and optimization of multipass heat exchangers (2006)”; Chemical Engineering and Processing

[4] Patel V.K., Rao R.V., “Design optimization of shell and tube heat exchanger using particle swarm optimization technique (2010)”; Applied Thermal Engineering

[5] Mohanty D.K., “Application of firefly algorithm for design optimization of a shell and tube heat exchanger from economic point of view (2015)”;International Journal of Thermal Sciences

[6] Masoud A et. al., “Economic optimization of shell-and-tube heat exchangers by a cuckoo-search-algorithm (2014)”; Applied Thermal Engineering

APPENDIX A: MATLAB CODE

```
function [f1 x] = ftrialr2 (x)
%     Ds = x(1);
%     do = x(2);
%     B  = x(3);

    a1 = 8000;
    a2 = 259.2;
    a3 = 0.93;

    n = 1;                                  %number of passes
    eff = 0.7;                              %Pump effficiency
    Nt = 60;                                %no. of tubes

    % tube side parameters
    mt = 18.80;
    Tci = 37.8;
    Tco = 76.7;
    rhot = 995.0;
    mut = 0.00358;                          %viscosity
    muwt = 0.00213;
    cpt = 2.05;
    kt = 0.13;
    Rft = 0.00061;
    st = 1.25*x(2);
    vt = (mt/(rhot*0.8*x(2).^2*pi/4))*n/Nt;   %velocity of fluid on tube side
    di = 0.8*x(2);

    Ret = rhot*vt*0.8*x(2)/mut;               %Reynold's number tube side
    ft = 0.079/(Ret^0.25);                    %Darcy friction factor
    Prt = mut*cpt/kt;                         %Prandtl number tube side
    % shell side parameters
    ms = 5.52;
    Thi = 199.0;
    Tho = 93.3;
    rhos = 850.0;
    cps = 2.47;
    mews = 0.0004;
    mewws = 0.00036;
    ks = 0.13;
    Rfs = 0.00061;
    ce = 0.12;                                %energy cost
    H = 7000;                                 %annual operating time in hours
    de = 4*(0.43*st.^2 - (0.5*pi*x(2).^2/4))/(0.5*pi*x(2));   %equivalent dia
    As = x(1)*x(3)*(1-x(2))/(1.25*x(2));      %shell side crooss section area
    vs = ms/(rhos*As);                       %velocity of fluid on shell side
    Res = ms*de/(As*mews);                   %shell side Reynold's number
    Prs = mews*cps/ks;                       %shell side Prandtl's number

    %Thermal Calculations
    hs = 0.36*(kt/de)*(Res^0.55)*(Prs^(1/3))*(mews/mewws)^0.14;     %shell
side heat transfer coefficient
     R = (Thi - Tho)/(Tco - Tci);               %correction coefficient
    P = (Tco - Tci)/(Thi - Tci);                %efficiency
```

```
    F = sqrt((R.^2+1)/(R.^2-1));                %correction factor
    LMTD = ((Thi - Tco) - (Tho - Tci))/(log((Thi-Tco)/(Tho-Tci)));
    Q = ms*cps*(Thi - Tho);
    L = 4.5;
    syms ht U A L
    [ht, U, A, L] = solve((ht == kt/di*(3.657 +
(0.0677*(Ret*Prt*((di/L).^1.33)).^1/3))/(1+0.1*Prt*(Ret*(di/L)).^0.3)), U ==
1/((1/hs)+Rfs+(x(2)/di)*(Rft+(1/ht))), A == Q/(U*F*LMTD), L ==
A/(pi*x(2)*Nt));

    if Ret < 2300
       ht = kt/di*(3.657 +
(0.0677*(Ret*Prt*((di/L).^1.33).^(1/3)))/(1+0.1*Prt*(Ret*(di/L)).^0.3));
       else if Ret > 2300 && Ret < 10000
       ht = kt/di*((1+di/L).^0.67*(ft/8)*(Ret -
1000)*Prt/(1+12.7*((ft/8).^0.5)*((Prt.^(2/3))-1)));
       else if Ret > 10000
          ht = 0.027*kt/do*(Ret.^0.8)*(Prt.^(1/3)).*(mewt/mewwt).^0.14;
       end
       end
   end

     U = 1/((1/hs)+Rfs+(x(2)/di)*(Rft+(1/ht)));
     A = Q/(U*F*LMTD);
     L = A/(pi*x(2)*Nt);

    %Pressure drop
    %tube side pressure drop
    p = 4;  %p = 2.5; %constant
    pt = 0.5*rhot*vt.^2*(L*ft/(0.8*x(2))+p)*n;

    %shell side pressure drop
    b0 = 0.72;
    fs = 2*b0*Res;
    ps = fs*(rhos*vs.^2/2)*(L/x(2))*(x(1)/de);
    f1 = (a1 + a2*A^a3)+ (ce*H*(mt*pt/rhot + ms*ps/rhos)/eff);
end

function [hist,searchdir] = runfmincon
    global hist
    hist.x = [];
    hist.fval = [];
    searchdir = [];
    x0 = [0.3 0.02 0.2]
    lb = [0.2 0.015 0.05 3];
    ub = [2 0.051 0.5 6];

    options = optimset('fmincon');
    options = optimset(options,'Display','Iter-detailed');
    options = optimset('PlotFcns',@optimplotfvalcust)
    figure
    options = optimset('PlotFcns',@optimplotxcust)
    options = optimset(options,'outputfcn',@outfun);
    nonlcon = [];
    [x,f1val] =  fmincon(@ftrialr2,x0,[],[],[],[],lb,ub,nonlcon,options)
end
```

Subsystem 2: Structural Analysis of the nozzle of a Heat Exchanger using Ansys

1. Problem Statement

A 3D model of a nozzle for minimizing the stress intensity incurred in the operation of a heat exchanger has to be formulated and optimized. The pressure, material and the physical properties of the nozzle are known. The required stress intensity and the deformation required to achieve the desired optimum conditions have been computed as a function of the design variables. The objective function is a function of the stress intensity.

2. Nomenclature

d_i	tube inner diameter (m)
d_o	tube outer diameter (m)
r	Inner radius of the nozzle (m)
θ	Taper angle (degrees)
t	Thickness of the nozzle (m)
x	The span from where the taper starts (m)

3. Model Formulation

The 3D modeling of the nozzle is done using solid works. The 4 design variables namely, the inner radius, taper angle, thickness of the nozzle and the span from where the taper starts are parameterized by declaring them as global variables. Only a portion of the shell is used as the study is done only on the nozzle and to add support to the support conditions. The application of boundary conditions on the shell simulates real world condition.
An internal pressure of 5 Mpa is applied as per ASME Codes. For the heat exchanger rating considered the above value of pressure is suited. Deformation is allowed so as to account for expansion due to thermal stresses and due to the loads acting on the Heat Exchanger which was also obtained from ASME Codes.

4. Boundary Conditions

The main cylinder of the Heat Exchanger and the location of the nozzle are fixed. It is due to the limitations imposed by internals of the Heat Exchanger. The constraints applied on the design variables are based on space considerations. The lower and upper bound values for the design variables have been selected by engineering judgment. Deformation allowance is given to account for loading conditions on the boiler due to internal pressure. Material properties are selected from ASME Boiler and Pressure Code Vessel.

Material properties are used of Structural Steel (Standard Material for Heat Exchanger).

Design Variables	Lower bound	Upper bound
Radius of the nozzle (r)	67.5	82.5
Taper angle (θ)	13.5	16.5
Nozzle Thickness(t)	90	110
Span (x)	90	110
Deformation (d1)	0.144	

3.1. FEA Model

A commercially available software, ANSYS Workbench, was utilized for modeling, meshing and FEA of the Heat Exchanger. In ANSYS Workbench 'Design Modeler' is a module for CAD modeling while 'Mechanical' is a module for generating the mesh and performing the FEA. Traditionally, a hexahedral mesh is computationally more efficient and preferable than the tetrahedral mesh. For creating hexahedral mesh in a body, sweep mesh is one of the methods which may be utilized.

ANSYS Mechanical normally mesh the source face with quadrilateral elements and then copy that mesh onto the target face, resulting a hexahedral mesh in the body. For creating an all-hexahedral finite element (FE) model of the heat exchanger , sweep mesh method was utilized in ANSYS Workbench. The heat exchanger as one part structure does not fulfil the topological requirements for sweeping and is therefore not amenable to hexahedral mesh. In order to make the heat exchanger amenable for sweep mesh, slicing and dicing technique was utilized for the creation of the geometry. Using the technique the un-sweepable heat exchanger was decomposed into several sweepable bodies. The sweepable multi-body heat exchanger was then glued together to make a single part. The gluing is also compulsory to ensure consistent nodes at the connecting faces of the sweepable bodies.

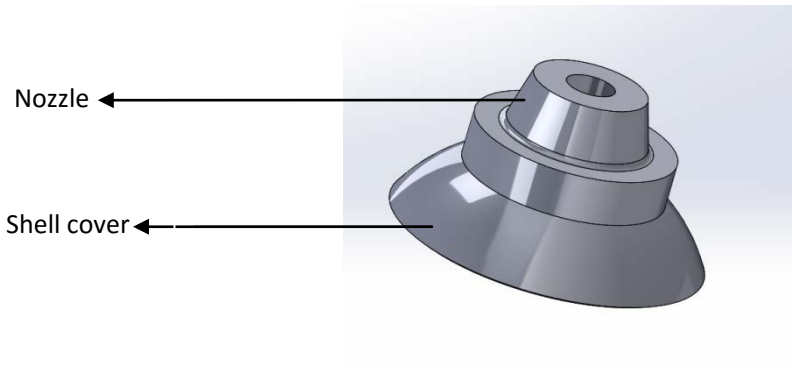

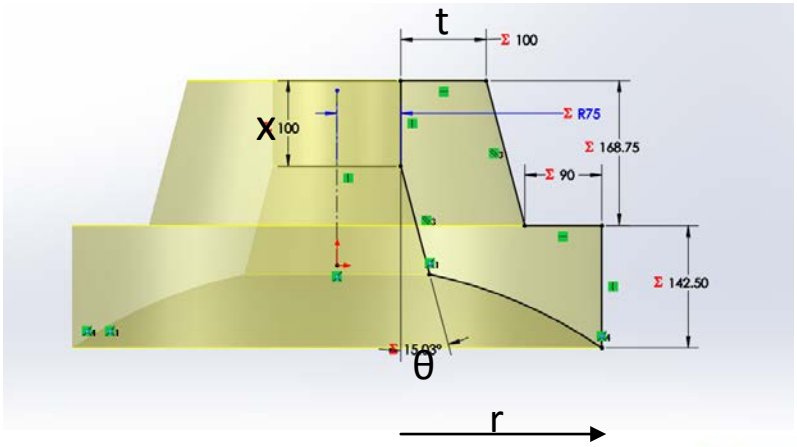

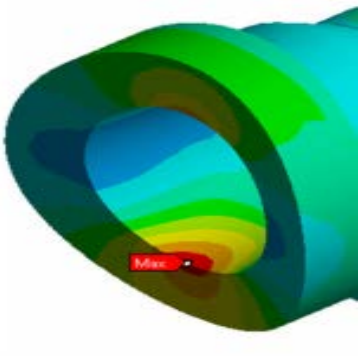

Maximum stress intensity on the edges

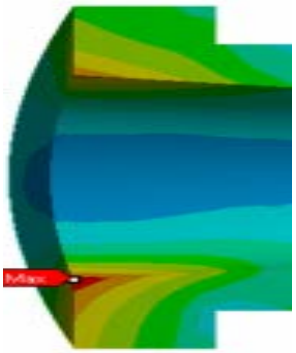

4. <u>Model Analysis</u>

The above model has four design variables. The objective function is a function of stress intensity. The stress intensity would be influenced by the size of the nozzle. Greater effective surface area around the edge would be desirable in terms of minimizing the stress intensity so as to eventually distribute the loads.

5. <u>Optimization Results</u>

To optimize the given model, a set of 100 design points are taken into consideration. From those design points optimal values are obtained which are well within constraints and minimize the objective.

Sensitivities charts:

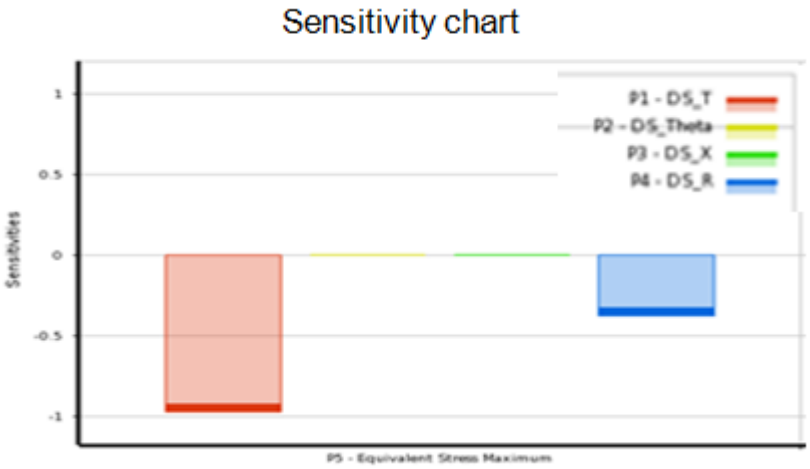

Thickness and radius are found to be most sensitive parameters

It shows the local sensitivity of each output parameter to the input parameters.

Conclusions from the sensitivity charts:

- The thickness and radius do decrease stress intensity and will require a closer examination to find the right trade-off between the input variables and stress intensity.
  If the nozzle's geometry is simplified to a cuboid or sphere the moment of inertia would vary by t^2 or t^3 respectively. The results obtained conform to this phenomenon.
- Taper Angle and Span have negligible effect on the stress intensity compared to the Thickness and Radius of the nozzle.

Goodness of fit:

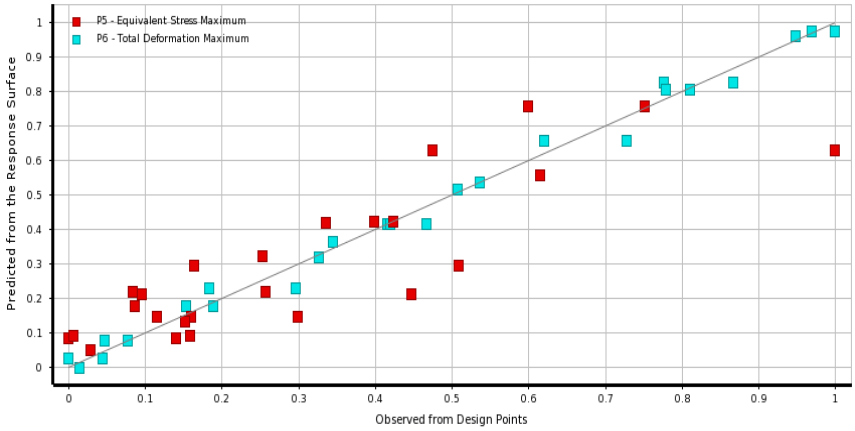

Both stress intensity and deformation values are obtained from the design points and the goodness of fit is obtained. The goodness of fit is the difference between assumed values and observed values. They can be used to measure the discrepancy.

Response Surface Curves:

The curves have thickness and stress intensity plotted with one other input variable as thickness is the most sensitive variable, it justifies to see the behaviour of the other input variables with respect to them.

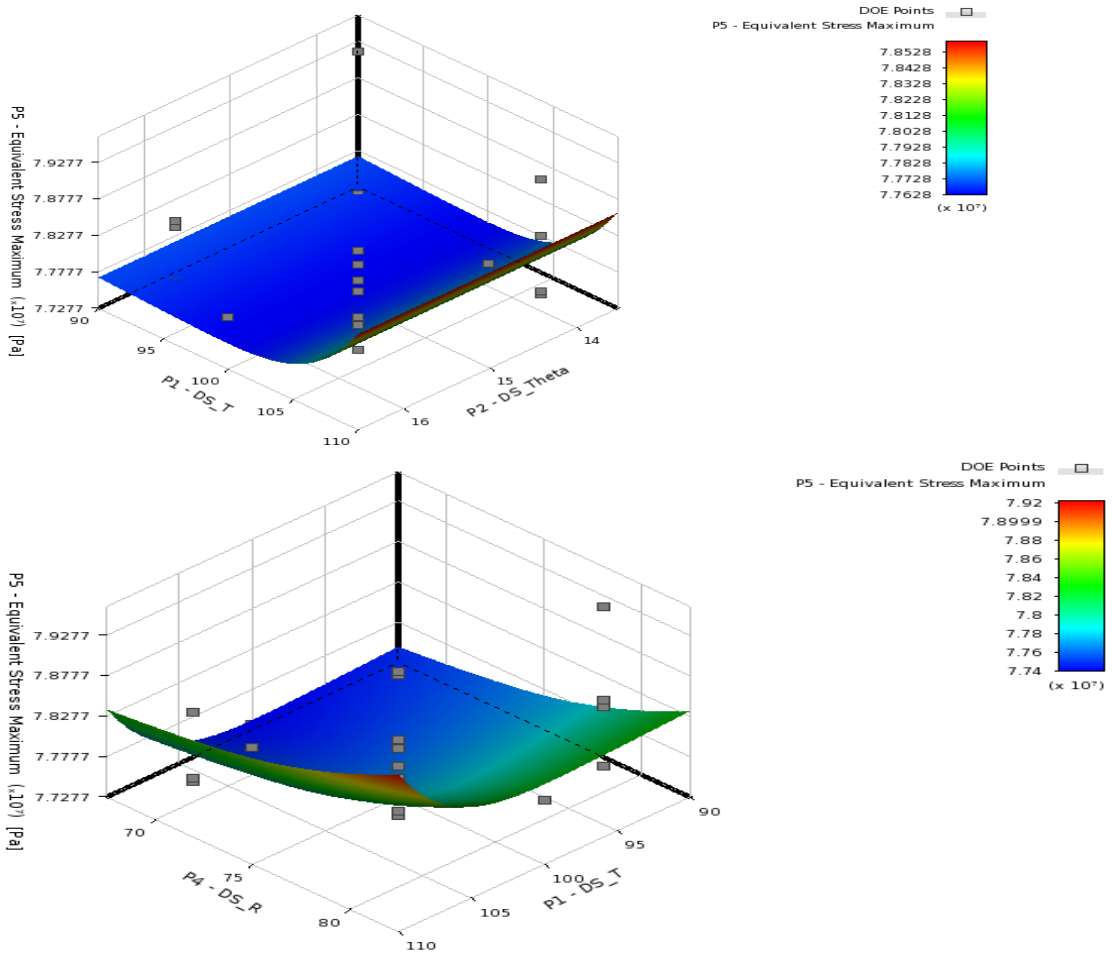

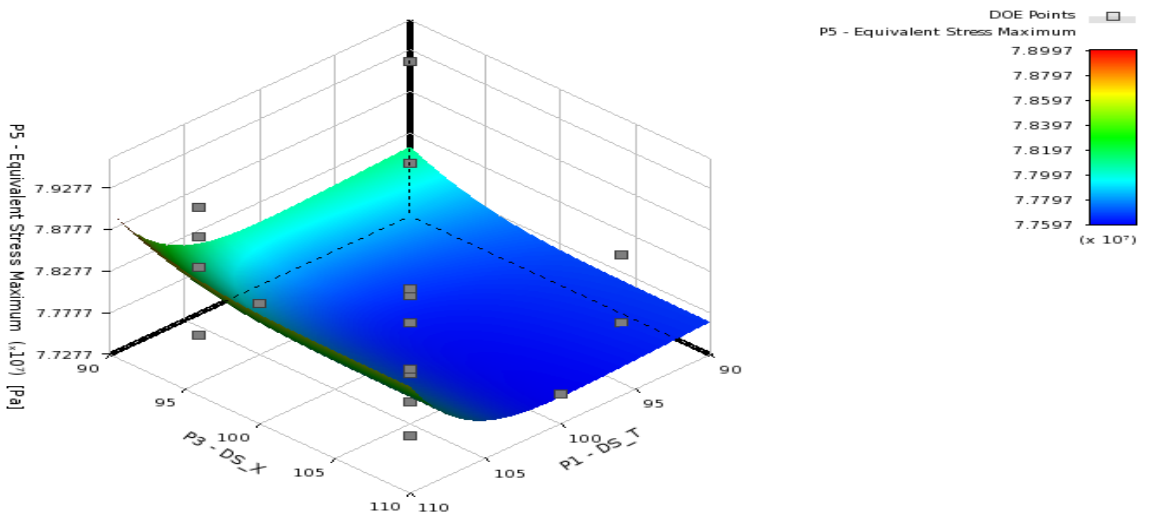

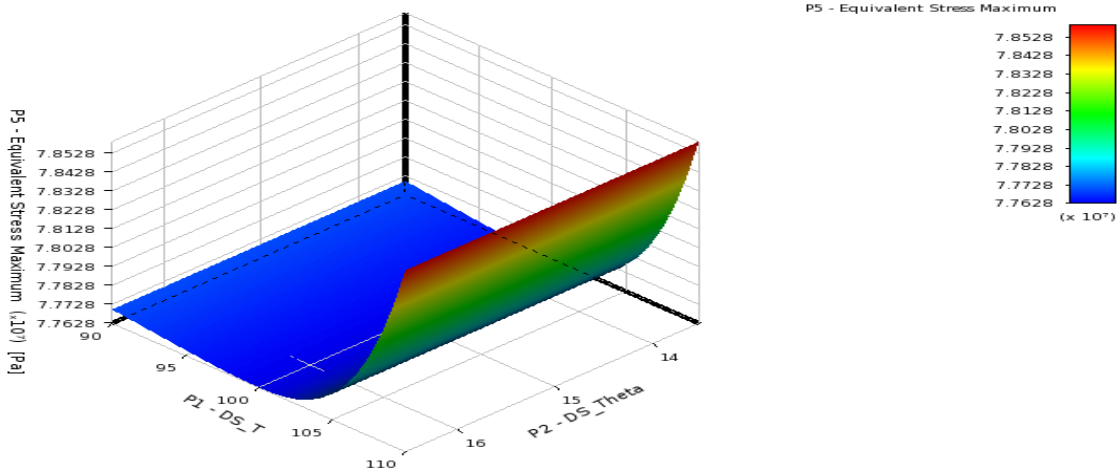

Pareto Graphs:

The algorithm used for solving is NLPQL which is a single objective algorithm used to minimize stress intensity.

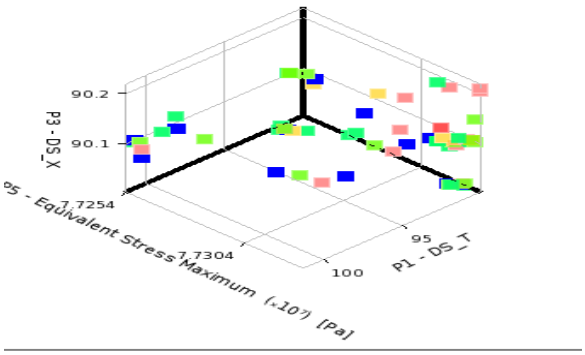

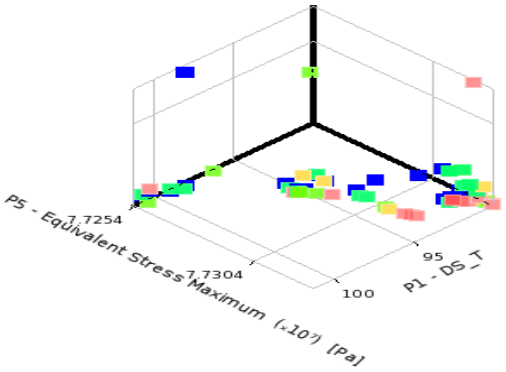

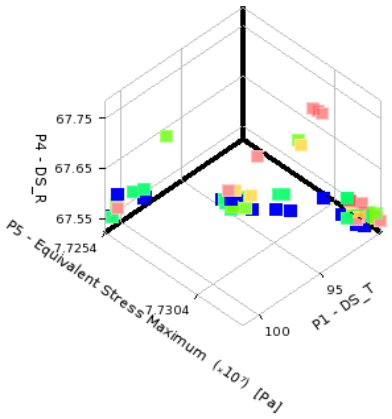

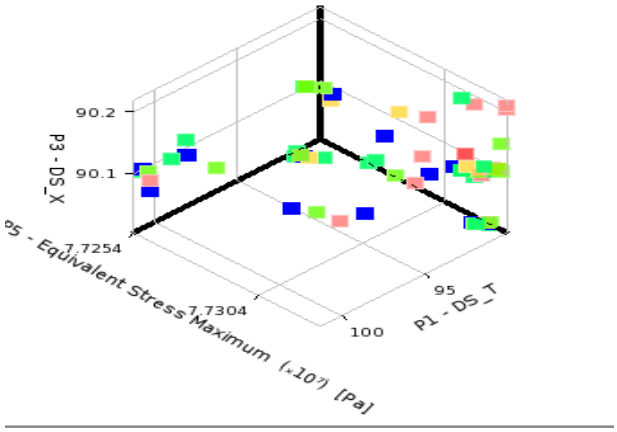

6. Optimized Results (Candidate Points)

	A	B	C	D	E	F	G	H	I
1	Reference	Name	P1 - DS_T	P2 - DS_Theta	P3 - DS_X	P4 - DS_R	P5 - Equivalent Stress Maximum (Pa)		P6 - Total Deform
2							Parameter Value	Variation from Reference	Parameter Value
3	◉	Starting Point	100	15.025	100	75	7.7628E+07	0.00 %	0.00014591
4	○	Starting Point (verified) DP 0					7.7654E+07	0.03 %	0.0001459
5	○	Candidate Point 1	100	15.025	102.38	67.5	7.7405E+07	-0.29 %	0.00014437
6	○	Candidate Point 1 (verified) DP 110					7.7458E+07	-0.22 %	0.00014428
7	○	Candidate Point 2	100	15.025	101.24	71.171	7.7486E+07	-0.18 %	0.00014508
8	○	Candidate Point 2 (verified) DP 111					7.7751E+07	0.16 %	0.00014489
9	○	Candidate Point 3	100	15.025	100.28	74.162	7.7588E+07	-0.05 %	0.00014571
10	○	Candidate Point 3 (verified) DP 112					7.759E+07	-0.05 %	0.00014552

From the optimization, 3 candidate points are obtained. The 3 candidates fall in the feasible region of the optimization problem. The points are also verified by Ansys to check if any deviation occurs. As seen, the percentage of variance is small and negligible.

As seen from the above table, the thickness 't' does not change, as 't' is the most sensitive variable. A small change in 't' would cause large change in stress intensity. The geometry of the nozzle is such that the value of 'θ' is closely related to 't' and 'r'. Variables 't' and 'r' being the most sensitive, the values of thickness and taper angle are optimized and constant for the candidate points.

From the given Heat Exchanger, candidate point 1 is the most ideal of the three and the variables are optimized.

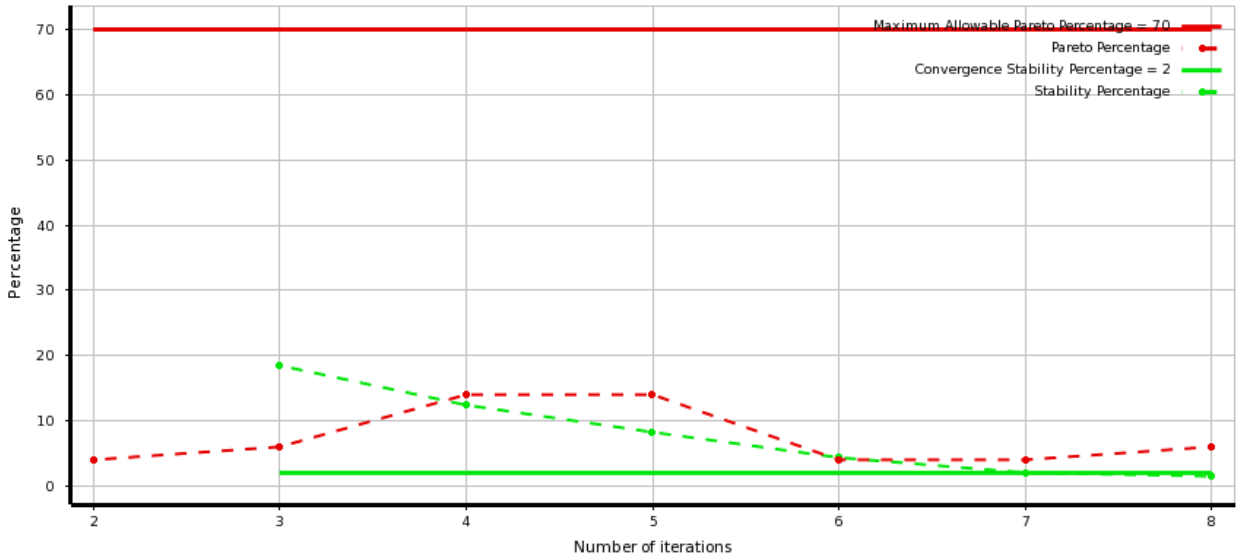

After 82 iterations, the solution converges

References

1. Adil, M., M.S. Dissertation 2012. Structural Analysis of Typical PWR Pressure Vessel (Effect of Cylindrical Thickness).
2. Design Exploration User's Guide. ASME Boiler and Pressure Vessel Code, Section II, Elementary Engineering Fracture Mechanics, 4th revised ed. Kluwer Academic Publishers, Eng. Design by analysis versus design by formula of high strength steel pressure vessels: a comparative study. Int. J. Pres. Ves. Pip. 82, 43–50. Dieter, G.E., 1987. Mechanical Metallurgy, 3rd ed. McGraw-Hill, USA. ESS, 1999.
3. Assessment and Management of Ageing of Major Nuclear Power Plant Components Important to Safety: PWR Pressure Vessels. European Committee for Standardization, EN 13445, Unfired Pressure Vessels – Part 3: Design, 2002.
4. Guerrero, M.A., Betegon, C., Belzunce, J., 2008. Fracture analysis of a pressure vessel made of high strength steel (HSS). Eng. Fail. Anal. 15, 208–219.
5. Haseeb, M., M.S. Dissertation 2014. Pressure Vessel Inlet Nozzle Strength Analysis Using ANSYS.
6. Theor. Appl. Fract. Mech., http://dx. doi.org/10.1016/j.tafmec.2014.12.001. Ramesh, K., 2007. E-Book on Engineering Fracture Mechanics.
7. IIT Madras, India. Shigley, J.E., 1986. Mechanical Engineering Design, 1st ed. McGraw-Hill, Singapore

Subsystem 3: Optimization of shell side parameters using Ansys Fluent

1. Problem Statement

This sub system involves optimization of shell side parameters especially the baffle parameters. This subsystem utilized optimized values from the Mathematical modelling subsystem. Analysis is performed using Ansys Workbench. The 3D model is created in Solidworks and analysed in Ansys Workbench using Fluent. Optimization is performed in DesignXplorer.

The trade-off that can be found using this subsystem is between pressure drop and heat transfer rate. Since Heat transfer rate is directly proportional to the output required and the pressure drop is directly proportional to energy spent in moving the fluid (Kerosene) from inlet to outlet, there will be a trade-off in amount of energy spent to amount of useful work obtained.

2. Nomenclature

∇p – Pressure gradient (Pa)
Δp – Pressure Difference (Pa)
a, b - Coefficients for quadratic fit
v - Fluid velocity (m/s)
S_i - Momentum Source or sink term in i^{th}direction
Δn - Length of the smaller domain used in porous resistance calculation (m)
μ - Fluid dynamic viscosity (kg/m.s)
α_p - Permeability of porous domain (m^2)
v_i - Velocity of the fluid in i^{th}direction (m/s)
C_2 - Inertial resistance coefficient
ρ - Density of fluid (Kg/m^3)

3. Model formulation

The objectives for this optimization are Minimization of shell side pressure drop and Maximization of shell side fluid heat transfer rate. The design variables that is to be optimized are Baffle spacing (B'), Baffle inclination (α), Baffle opening (B_o). The constraints are given in the form of upper and lower bounds for the design variables [1]. The optimized parameters that is considered from the mathematical subsystem are Shell inside diameter (Ds), Length of the Heat exchanger (L), Tube diameter (d_o).

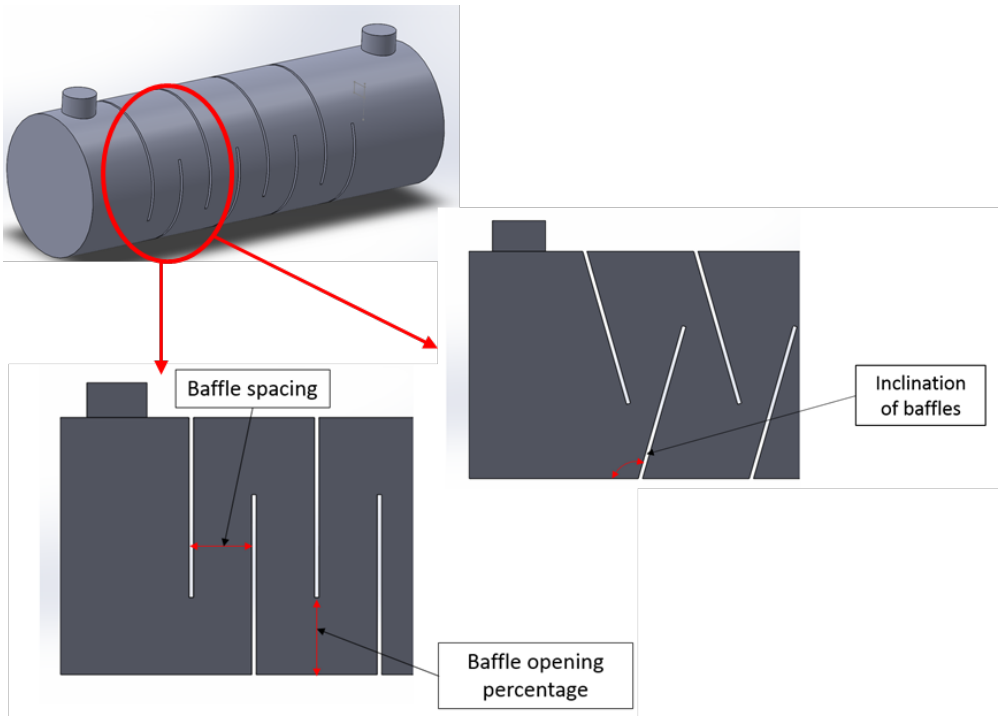

Figure3.1:3D model and Design variables

Parameter	Lower bound	Upper bound
Baffle spacing (m)	0.35	0.85
Angle (degrees)	90	120
Percent open (%)	25	45

Table 3.1: Lower and upper bounds for variables

The 3D model was created using Solidworks and since the model is symmetric, only a half of the geometry was created to reduce the element count.

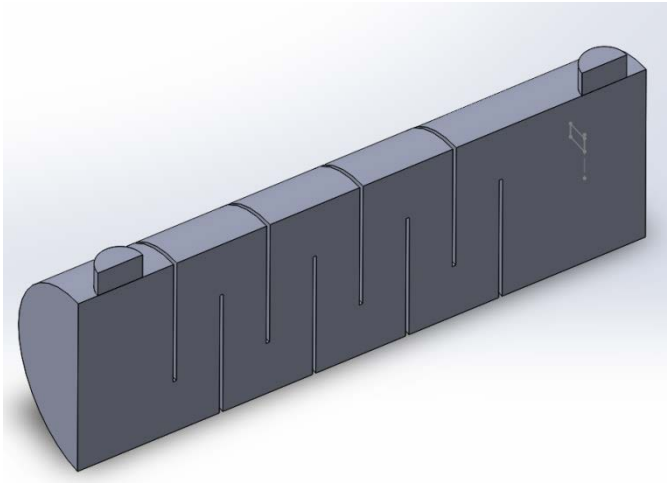

Figure3.2:3D CAD model of Geometry

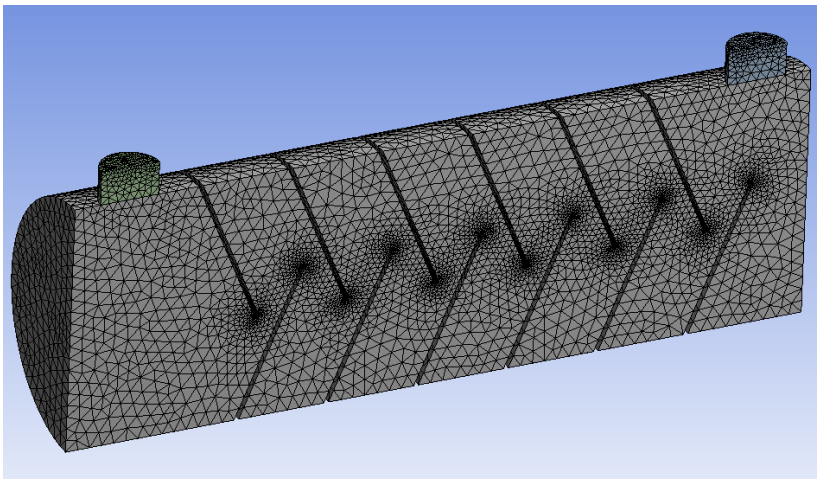

Figure3.2: Mesh generated for the heat exchanger

The crucial part in modelling of the shell side geometry is to consider the tubes and considering the tube geometry as it is would increase the cell count and hence the computational time because of the necessity to maintain a very small mesh near the walls to capture the very high velocity and temperature gradient. So an alternate porous resistance formulation is used. Here, a system resistance curve which is available in the form of pressure drop against velocity through the porous component, can be extrapolated to determine the coefficients for the porous media. The resistance is anisotropic, so different resistance co-efficient for different directions is determined.

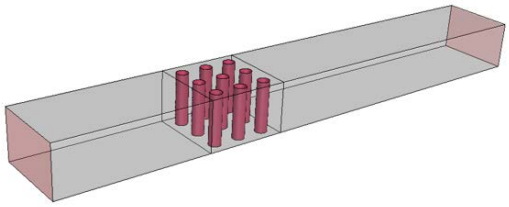

Figure3.3a: Geometry for resistance calculation in Y and Z direction

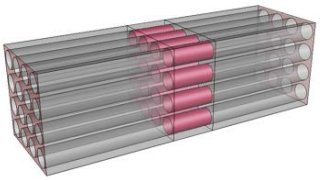

Figure3.3b: Geometry for resistance calculation in X direction

Figure3.3: Geometry for resistance calculation

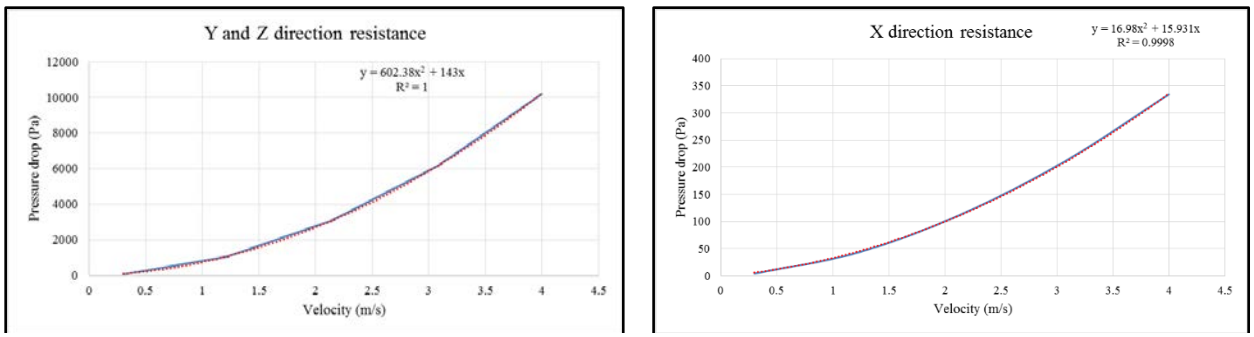

Figure3.3: System resistance curveResistance

The resistance coefficients for the system is determined by using the following procedure from Ansys fluent theory guide [2].

The system resistance curve is fitted onto a

$$\Delta p = av^2 - bv$$

Rewriting pressure drop as a sink term in the momentum equation we get

$$\nabla p = -S_i$$

Or

$$\Delta p = -S_i \Delta n$$

For a simple homogenous porous media

$$S_i = -(\frac{\mu}{\alpha_p} v_i + C_2 \frac{1}{2} \rho |v| v_i)$$

This equation becomes

$$a = C_2 \frac{1}{2} \rho \Delta n$$

And

$$b = \frac{\mu}{\alpha_p} \Delta n$$

		X direction	Y and Z direction
Inertial resistance	C_2	0.1958	4.5574
Viscous resistance	$\frac{1}{\alpha_p}$	195232.8	1149517.7

Table 3.2: Inertial and viscous resistances for different directions

These resistance values given to replicate the effects for tubes. A Heat sink model is used for modelling the heat transferred in the shell section.

The various assumptions and properties used for creating the numerical model is described in table 3.3

Property	Value
Density (Kg/m^3)	850
Specific Heat (J/Kg.K)	2470
Thermal Conductivity (W/m.K)	0.13
Viscosity (kg/ms)	0.0004

Table 3.3: Material properties for Kerosene [3]

Location	Value
Inlet mass flow rate (Kg/s)	5.52
Inlet Temperature (K)	472.15
Outlet gauge pressure (Pa)	0

Table 3.4: Boundary conditions for the simulation

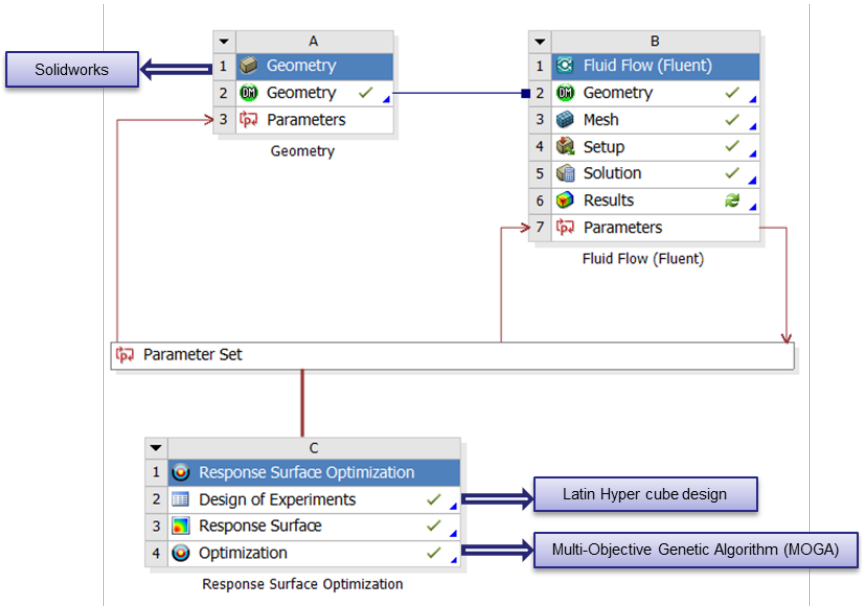

Figure3.4: System schematic

4. Design of experiments

While simulating a fluid flow coupled with heat transfer, there will be nonlinearities and noise in the response measured. This was eliminated by using Latin Hypercube space filling design with 100 design points.

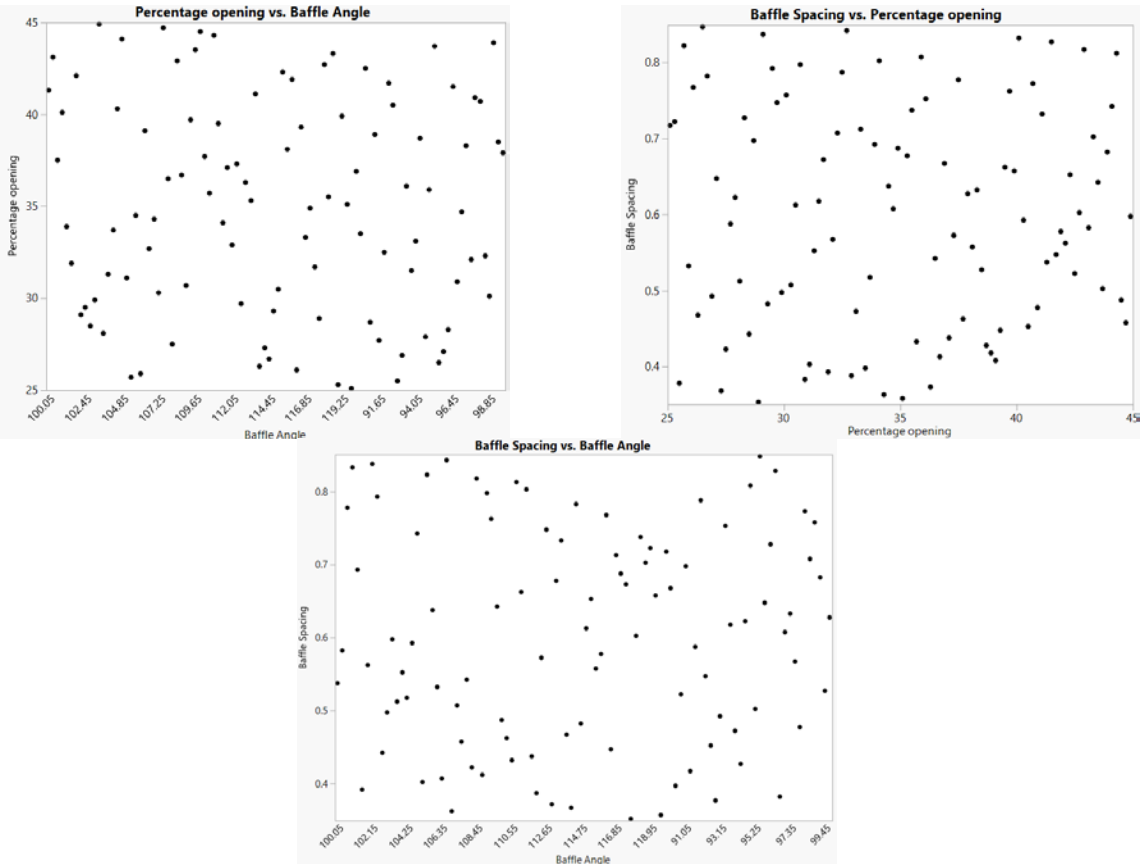

Figure3.4: Scatter plot showing different design points for design variables

5. <u>Response surface modelling</u>

A Kriging Metamodel is used for fitting the design points unto a model. A sufficiently accurate model is obtained which is shown from the goodness of fit as the observed values from design points align well with the predicted value from response surface.

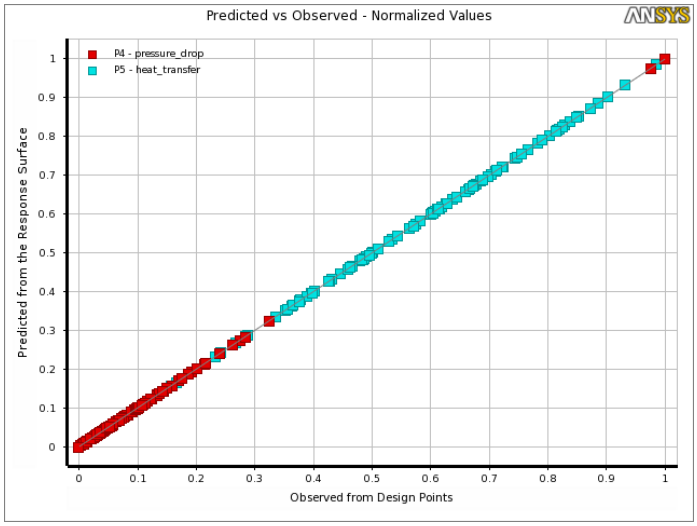

Figure3.5: Goodness of fit plot

The response surface plots for the pressure drop and heat transfer is plotted and shown in figure 3.6

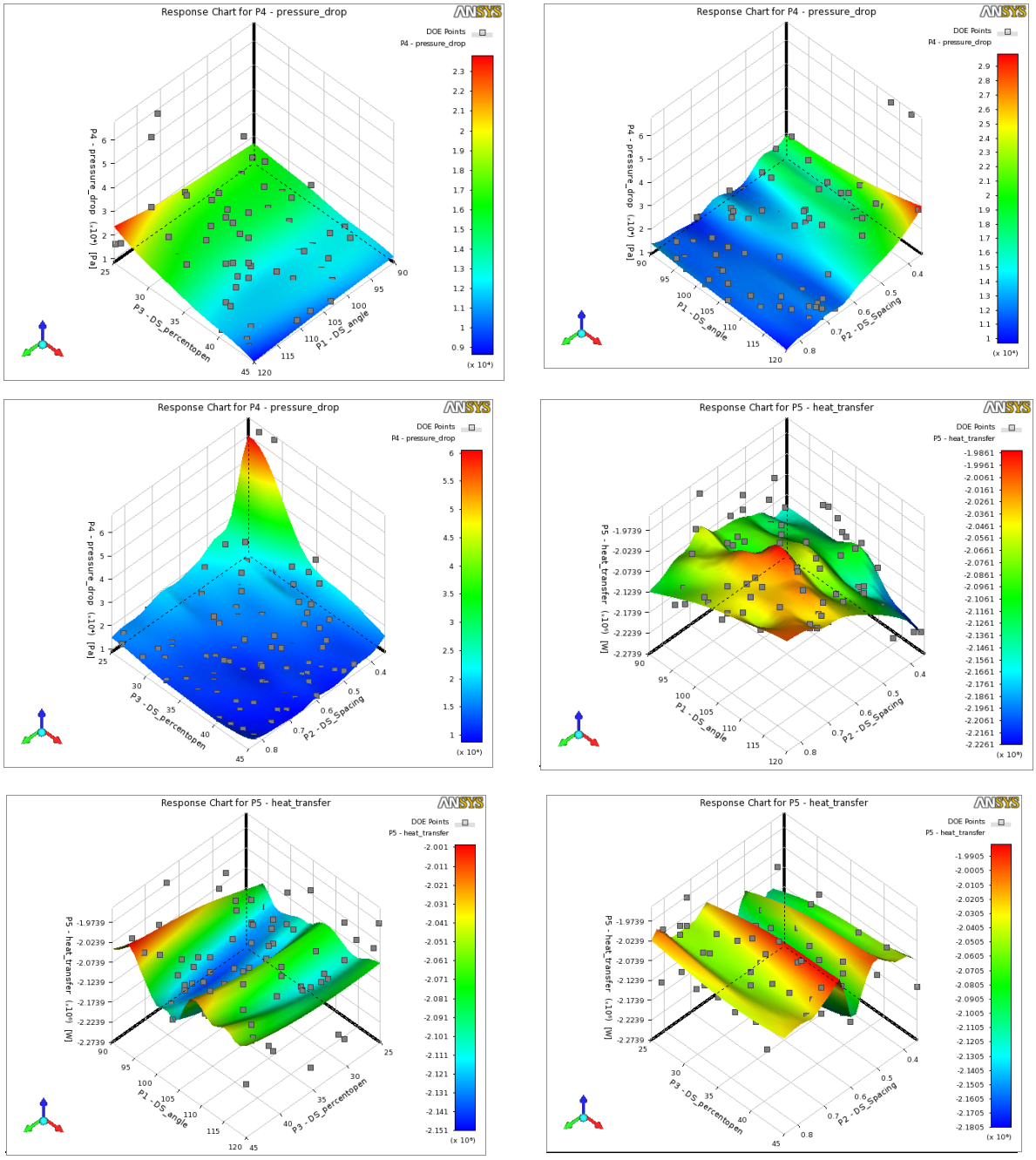

Figure3.6: Response surface plots

The globalsensitivity values of the variables are plotted using a bar chart in figure 3.7

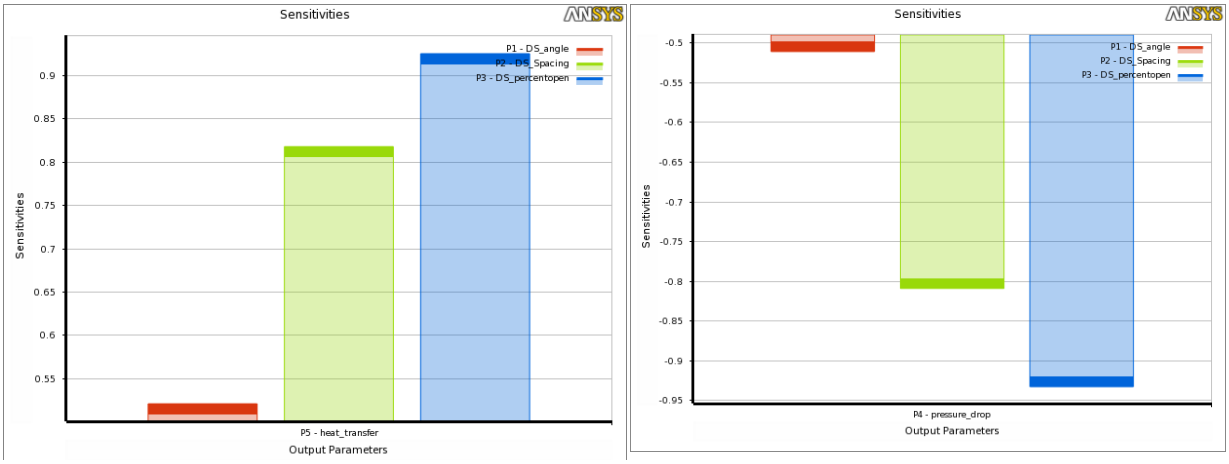

Figure3.6: Global sensitivity plots

It can be observed from the sensitivity and the response surface that both pressure drop and heat transfer rate is most sensitive to percentage of opening of baffles followed by baffle spacing. This is logical because the opening of the baffles increases the flow path which in turn increases the pressure drop i.e., the energy required to transport the fluid from inlet to outlet.

For heat transfer rate, the percentage opening of the baffle increases again increases the heat transfer rate because of increase in the flow path and the same goes for the spacing. It is to be noted that angle of inclination of the baffles plays a not so important role in deciding the pressure drop and heat transfer rate.

The sensitivity plots of the heat transfer is positive and that of pressure drop is negative which implies that there is a trade-off between both the objectives, which is determined in the next section.

6. Optimization

A multi-objective Genetic algorithm (MOGA) was used for optimization. The optimization solution converges after 604 evaluations as shown in figure 3.7

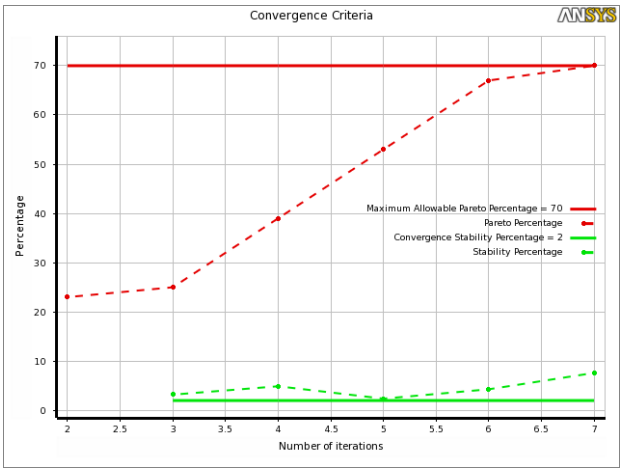

Figure3.7: Convergence plot

The Pareto front showing the trade-off between different parameters as shown in the figure 3.8 and 3.9

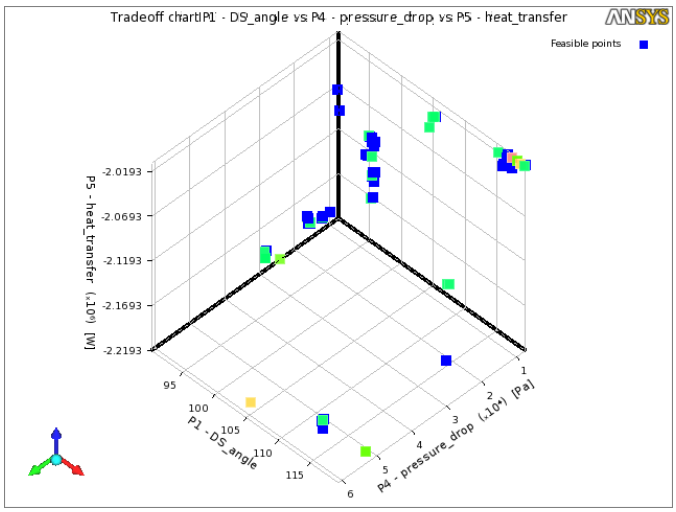

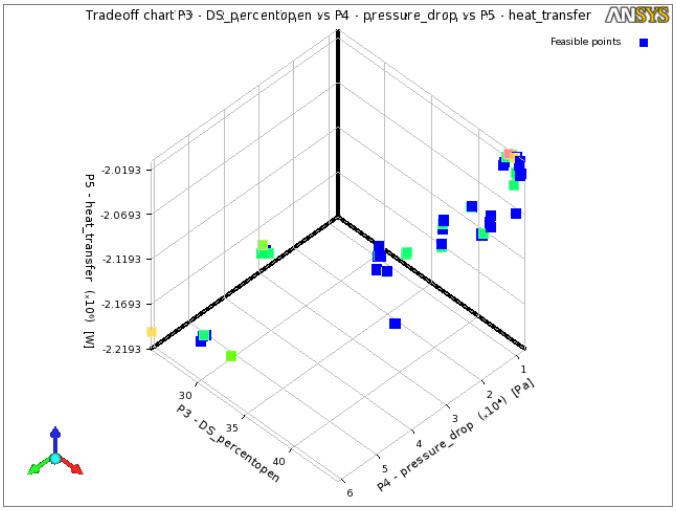

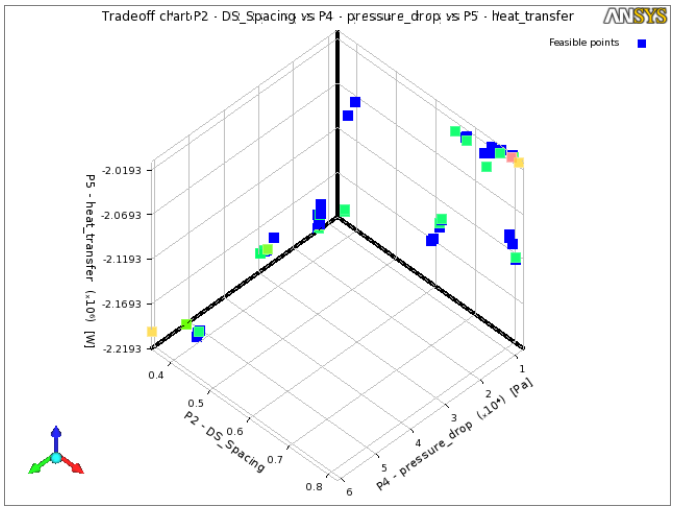

Figure3.8: Pareto surface plots of design variables

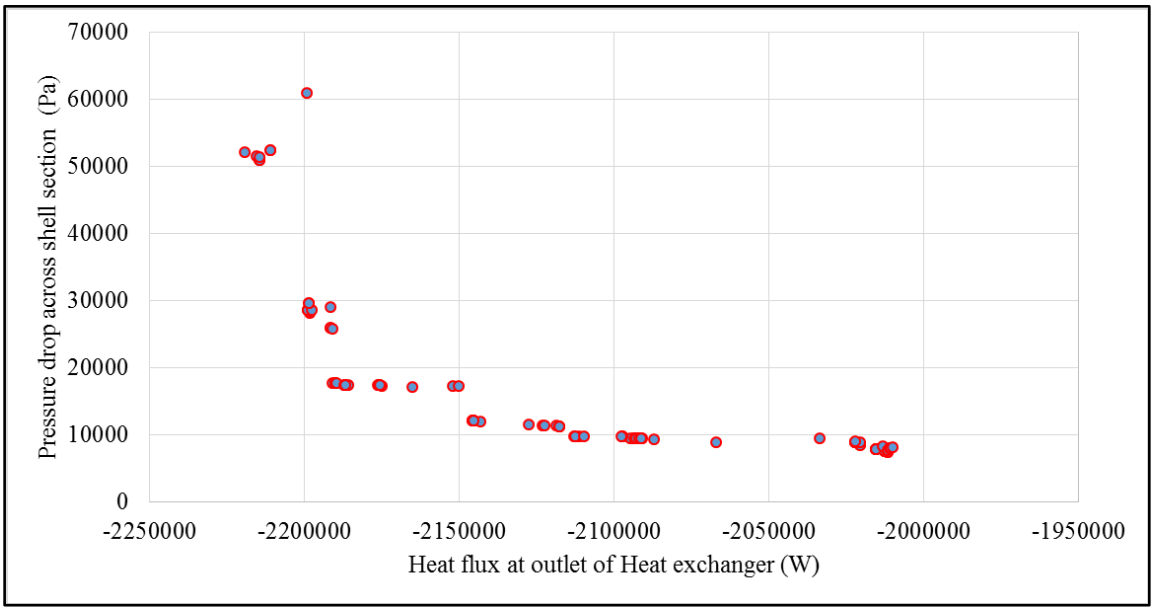

Figure3.8: Pareto plot of objectives

The Pareto plot shows the trade-off between heat flux at the outlet and the pressure drop in the graph of the feasible point. The trade-off is seen clearly from the trend of the curve. For achieving a maximum heat transfer rate (low heat flux at outlet), a high pressure drop is required i.e., a high input of energy is required for achieving a high heat transfer rate and the vice versa.

7. Conclusion

Three Candidate points are selected from the feasible point and is verified by running a trial run. I is seen that only a minor variation is observed except for the pressure drop of third candidate point which is 11 percentage deviation from the predicted value.

# Name	Angle (degrees)	Spacing (m)	Percentopen (%)	Pressuredrop (Pa)	Percentage variation	Heat transfer (W)	Percentage variation
Candidate Point 1	91.15	0.392	33.0	17796	2.144	-2190886	4.657
Candidate Point 1 (verified)	91.15	0.392	33.0	18186		-2093392	
Candidate Point 2	97.84	0.63	37.81	12092	-3.262	-2145486	2.379
Candidate Point 2 (verified)	97.84	0.631	37.8	11710		-2095640	
Candidate Point 3	117.15	0.353	38.0	25914	-11.107	-2191617	-0.427
Candidate Point 3 (verified)	117.15	0.353	38.0	23323		-2201007	

Table 3.5: Candidate points

References

1. K. Raj and S. Ganne, “Shell side numerical analysis of a shell and tube heat exchanger considering the effects of baffle inclination angle on fluid flow using CFD,” *THERM SCI Thermsci THERMAL SCI Thermal Science*, vol. 16, no. 4, pp. 1165–1174, 2012.
2. “FLUENT 6.3 User's Guide - 7.19.6 User Inputs for Porous Media,” *FLUENT 6.3 User's Guide - 7.19.6 User Inputs for Porous Media*. [Online]. Available at: https://www.sharcnet.ca/software/fluent6/html/ug/node276.htm. [Accessed: 25-Apr-2016].
3. V. Patel and R. Rao, “Design optimization of shell-and-tube heat exchanger using particle swarm optimization technique,” *Applied Thermal Engineering*, vol. 30, no. 11-12, pp. 1417–1425, 2010.
4. R. MUKHERJEE, “Effectively Design Shell-and-Tube Heat Exchangers,” *University of Thessaly*. [Online]. Available at: http://www.mie.uth.gr/ekp_yliko/cep_shell_and_tube_hx.pdf. [Accessed: 25-Apr-2016].

System Level Integration

The three sub-systems were modeled so as to obtain an overall optimized model of the shell and tube heat exchanger. The outputs computed in the 1st subsystem i.e. the Mathematical model have been used in the subsequent subsystems to evaluate the remaining design variables. As a result from the optimization of the three subsystems, a total of 10 design variables have been optimized, thus presenting a completely optimized shell and tube heat exchanger design.

Since, the optimized values of the Mathematical model were used to optimize completely independent design variables in the remaining two sub-systems, there would not be any tradeoffs between the subsystem optimizations.